

Elastic network normal mode dynamics reveal the GPCR activation mechanism

Dikla Kolan, Gennadiy Fonar, and Abraham O. Samson*

Faculty of Medicine in the Galilee, Bar Ilan University, Safed, Israel

ABSTRACT

G-protein-coupled receptors (GPCR) are a family of membrane-embedded metabotropic receptors which translate extracellular ligand binding into an intracellular response. Here, we calculate the motion of several GPCR family members such as the M2 and M3 muscarinic acetylcholine receptors, the A_{2A} adenosine receptor, the β_2 -adrenergic receptor, and the CXCR4 chemokine receptor using elastic network normal modes. The normal modes reveal a dilation and a contraction of the GPCR vestibule associated with ligand passage, and activation, respectively. Contraction of the vestibule on the extracellular side is correlated with cavity formation of the G-protein binding pocket on the intracellular side, which initiates intracellular signaling. Interestingly, the normal modes of rhodopsin do not correlate well with the motion of other GPCR family members. Electrostatic potential calculation of the GPCRs reveal a negatively charged field around the ligand binding site acting as a siphon to draw-in positively charged ligands on the membrane surface. Altogether, these results expose the GPCR activation mechanism and show how conformational changes on the cell surface side of the receptor are allosterically translated into structural changes on the inside.

Proteins 2014; 82:579–586. © 2013 Wiley Periodicals, Inc.

Key words: GPCR; G-protein-coupled receptor; normal modes; muscarinic; adrenergic; CXCR4; adenosine.

INTRODUCTION

Guanine nucleotide binding protein (G-protein) coupled receptors (GPCR) comprise a family of transmembrane proteins that are involved in the transfer of extracellular signals to the cell interior. The GPCR superfamily shares a common structural feature that consists of seven transmembrane helices (TM1-7), which are connected by three extracellular and three cytoplasmic loops. These metabotropic receptors are activated by binding a wide variety of extracellular molecules, peptides, nucleotides, and amino acids. GPCRs are known to play important roles in various types of neuronal, cardiovascular, gastrointestinal, inflammatory, and other diseases, making the receptors ideal targets for new drug development. The importance of the GPCRs is reflected by the fact that they constitute the largest family of protein in the human genome, and that nearly 50% of all recently launched drugs target receptors from this family.² The last recent years have seen an explosion in the knowledge of GPCR structures with the advent of the M2 and M3 muscarinic acetylcholine receptor, ^{3,4} the CXCR4 chemokine receptor,⁵ the A_{2A}-adenosine receptor, 6 and the β_{2} -adrenergic receptor. 7

Muscarinic acetylcholine receptors (mAChR) are a family GPCRs that mediate the response of acetylcholine released from parasympathetic presynaptic vesicles. mAChR consist of five subtypes (M1–M5), of which M1, M3, and M5 subtypes are coupled with G_q proteins, while M2 and M4 subtypes are coupled with G_i and G_o proteins. Muscarinic receptors bind several agonists such as acetylcholine and muscarine, as well as antagonists like 3-quinuclidinyl-benzilate and N-methylscopolamine.

The CXCR4 chemokine receptor (CXCR4) is a GPCR that is activated exclusively by the chemokine ligand SDF-1 and couples primarily through G_i proteins. ⁹ CXCR4 has been associated with more than 23 types of

Additional Supporting Information may be found in the online version of this article.

Abbreviations: $A_{2A}AR$, A_{2A} adenosine receptor; β_2AR , β_2 adrenergic receptor; CXCR4, CXCR4 chemokine receptor; G-protein, guanine nucleotide-binding protein; GPCR, G-protein-coupled receptor; mAChR, muscarinic acetylcholine receptor

Grant sponsor: Marie-Curie CIG; Grant number: 322113; Grant sponsor: Katz Foundation.

*Correspondence to: Abraham O. Samson, Bar Ilan University, 8, Henrietta Szold str., Safed 14310, Israel. E-mail: avraham.samson@biu.ac.il

Received 10 February 2013; Revised 28 August 2013; Accepted 13 September 2013 Published online 1 October 2013 in Wiley Online Library (wileyonlinelibrary. com). DOI: 10.1002/prot.24426

© 2013 WILEY PERIODICALS, INC. PROTEINS 579

cancers, where it promotes metastasis, angiogenesis, and tumor growth or survival. 10 In addition, T-cell tropic HIV-1 uses CXCR4 as a coreceptor for viral entry into host cells.11

The β_2 -adrenergic receptor (β_2AR) is a GPCR that is activated by catecholamines, especially epinephrine and norepinephrine. β₂ARs reside predominantly in smooth muscle throughout the body, where they are targeted by many drugs to treat asthma, preterm labor, hypertension, and other pathologies. 12

The A_{2A}-adenosine receptor (A_{2A}AR) is one of four GPCR activated by adenosine enumerated A₁, A_{2A}, A_{2B}, through A₃.¹³ Together, these receptors regulate pain, cerebral blood flow, basal ganglia functions, respiration, and sleep.

The only structure representative of the GPCR family prior to Kobilkas ingenious idea of crystallizing membrane protein with lysozyme, was that of rhodopsin. 14 Rhodopsin is the best characterized GPCR which binds retinal in the eye where it is activated by light. 15

Normal mode analysis (NMA) is one of the standard techniques for studying long time dynamics and, in particular, low-frequency motion. In contrast to molecular dynamics, normal mode analysis provides a very detailed description of the dynamics around a local energy minimum. Even with its limitations, such as the neglect of the solvent effect, the use of harmonic approximation of the potential energy function, and the lack of information about energy barriers and crossing events, normal modes have provided much useful insight into protein dynamics. Over the past years, several techniques have been described to calculate large-scale motions using full atomic normal-mode analysis with rigorous force fields, 16,17 simplified NMA using a uniform harmonic potential, 18–20 as well as low resolution normal-mode analysis.^{21–24} Based on these techniques, several programs and modules to calculate normal modes have been released, such as ANM,^{23,25} ElNémo,²⁶ GROMACS' NMA module,²⁷ NOMAD,²⁸ and STAND.¹⁷ These programs, as well as others have been used to calculate the mechanical motion of several biomolecules.^{29–37} Most noteworthy is an article by Bahar and coworkers³⁵ in which normal modes were calculated for rhodopsin and other membrane proteins. In their article, the mechanical features of rhodopsin which were predicted using Gaussian and anisotropic normal modes were consistent with experimental data. Finally, normal mode analyses of membrane proteins were extensively reviewed in a recent publication by Bahar et al.³⁸

Here we report elastic network normal mode calculations of the β₂-adrenergic receptor, the CXCR4 chemokine receptor, the A_{2A}-adenosine receptor, and the M2 and M3 muscarinic acetylcholine receptors. To our knowledge, this is the first comprehensive normal mode analysis of these GPCRs. Although earlier studies did calculate the normal modes of rhodopsin, another member of the GPCR family,^{33–37} structural differences between rhodopsin and other members of the GPCR family (i.e., covalently bound ligand, chromophore lid, etc.) oblige a comprehensive study of the newly determined structures. Our calculations reveal that ligand binding and vestibule dilation is associated with cavity formation and pivotal motion of the cytoplasmic domain. Cavity formation in the cytoplasmic domain is in part responsible for the binding of free G-protein, and sheds light on the activation mechanism of GPCRs.

COMPUTATIONAL METHODS

Normal mode calculation

Elastic network normal modes of GPCRs, including the M2 muscarinic acetylcholine receptor PDB ID 3UON,³ the M3 muscarinic acetylcholine receptor PDB ID 4DAJ,4 the β₂-adrenergic receptor PDB ID 2RH1,⁷ rhodopsin PDB ID 1F88, 14 the A_{2A}-adenosine receptor PDB ID 3EML, 6 and the CXCR4 chemokine receptor⁵ were calculated using several computational tools namely ElNémo, ²⁶ NOMAD-Ref, 28 and STAND. 17 For all structures, normal modes were calculated with and without the T4L lysozyme domain. For the CXCR4 chemokine receptor, the unstructured C-terminus was truncated at residue 310. For ElNémo, the default parameters used were C_{α} coarse graining, ENM cutoff of 8 Å, minimum perturbation amplitude DQMIN of -100, maximum perturbation amplitude DQMAX of 100, and amplitude increments DQSTEP of 20. For NOMAD-Ref, the sparse metric solver method was utilized with C_{α} coarse graining, default distance weight parameters for elastic constant of 5 Å, ENM cutoff values of 10 Å, and average RMSD for output trajectories of 1 Å. For STAND, the default parameters were C_{α} coarse graining, ENM cutoff of 9 Å, average RMSD in output trajectories of 1 Å. ElNémo, STAND, and Nomad use cutoff values of 8, 9, and 10 Å, respectively, to generate the elastic network. These cutoff values are the recommended default values, and as such were not changed. For STAND, normal modes were calculated in both Cartesian coordinate space (TIR) and torsion angle space (REA). The methods are very different in that STAND (REA) minimizes the structure and then calculates modes in single bond torsion-angle space whereas STAND (TIR), ElNémo, and Nomad-Ref avoid minimization by using Tirion modes 19 and then calculate modes in Cartesian coordinate space. The STAND program was a generously provided by Prof. Michael Levitt of Stanford University. In all cases, the lowest 25 modes were calculated. The first six trivial normal modes are discarded because they represent only translation and rotation.

Multiple sequence alignment of GPCRs was performed using Clustal W.39 This sequence alignment was used in the alignment of the normalized mean square displacement of C_{α} atoms (RMSD) associated with the slowest

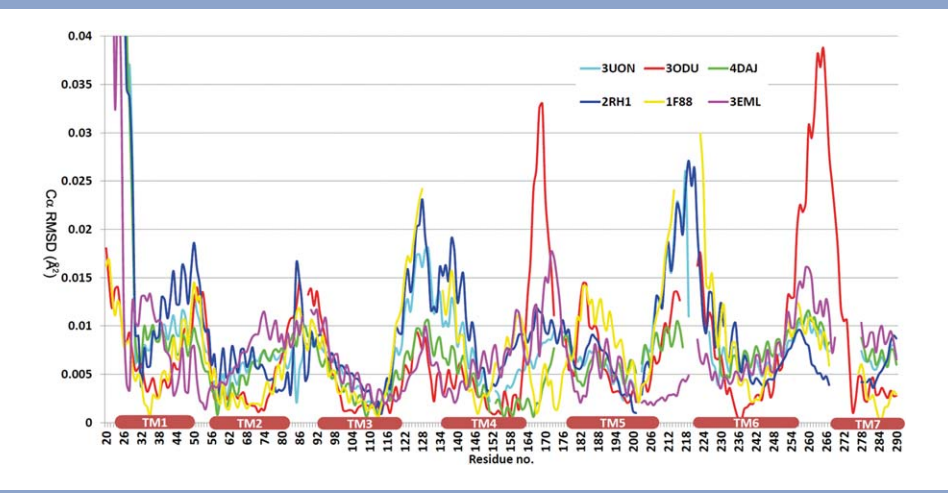


Figure 1

Normal modes dynamics of GPCRs. Shown are the root mean square displacement (RMSD) values of C_{α} atoms of the M2 and M3 muscarinic acetylcholine receptors (PDB ID: 3UON and 4DAJ), the β_2 -adrenergic receptor (PDB ID: 2RH1), the A_{2A} -adenosine receptor (PDB ID: 3EML), the CXCR4 chemokine receptor (PDB ID: 3ODU), and rhodopsin (PDB ID: 1F88) associated with the slowest mode calculated using ElNémo. Note the relatively small deviation of TM helices, and the relatively large deviation of intracellular and extracellular loops. The numbering of the residues follows that of the M2 muscarinic acetylcholine receptor (see sequence alignment in the Supporting Information).

mode of GPCR residues. Intermolecular RMSD was calculated using the Pymol program.

Pocket calculation

To calculate pockets, the program Ligsite CSC was utilized.⁴⁰ The 10 largest pockets were calculated for all GPCR structures, distorted along the lowest frequency normal mode, using a probe radius of 1.8 Å, and a grid size of 1 Å.

Electrostatic potential

The electrostatic potential of the M2 and M3 muscarinic acetylcholine receptor, PDB ID 3UON³ and 4DAJ,⁴ respectively, as well as the A2A-adenosine receptor and β₂-adrenergic receptor, PDB ID 2RH1,⁷ were calculated using the Adaptive Poisson–Boltzmann Solver (APBS)⁴¹ of the VMD program.⁴²

RESULTS

Normal modes of GPCR

The lowest frequency elastic network normal mode motion of the M2 and M3 muscarinic acetylcholine receptors, the β₂-adrenergic receptor, the A_{2A}-adenosine receptor, the CXCR4 chemokine receptor, and rhodopsin calculated using ElNémo is shown in Figure 1. To avoid data redundancy, all tables and figures presented in this study were prepared using data from ElNémo alone, and identical data obtained using Nomad and STAND are not shown. Also, the modes discussed and displayed in this study correspond to the slowest modes, unless otherwise indicated. The motion amplitude was not scaled, and retains the original values calculated using normal modes. The motion is shown to be relatively small in the TM α -helices, and relatively large in their interconnecting loops. The calculated motion of the lowest-frequency normal mode of the GPCRs correlate nicely with an average pairwise correlation coefficient of 0.8 for the C_{α} displacement RMSD measure (Table I, upper right triangle). On average, normal modes calculated in Cartesian coordinate space display a slightly lower correlation coefficient of 0.77 compared to those calculated in torsion space. 43 The calculated motion involves contraction of the ligand binding pocket and of the vestibule leading to the binding site (Fig. 2). Contraction of the ligand binding pocket and vestibule involves all TM helices and in particular TM1, TM6, and TM7. This is in agreement with experimental data which shows that dilation of the cytoplasmic vestibule involves translation of TM1 (3 Å), TM5 (2 Å), TM6 (14 Å), and TM7 (3 Å) between the active and inactive forms of the \(\beta_2\)-adrenergic receptor, and constriction of the extracellular ligand binding site involves translation of TM1 (4 Å), TM5 (2 Å), TM6 (3

RMSD of GPCS structures and C_{α} displacements

$\begin{array}{c} RMSD\ (\mathring{A}) \backslash C_{\alpha} \\ displacement\ RMSD \end{array}$	3UON	30DU	4DAJ	2RH1	3EML	1F88
3U0N	_	0.68	0.98	0.98	0.79	0.34
30DU	1.8	_	0.64	0.65	0.62	0.45
4DAJ	0.6	1.8	_	0.97	0.86	0.26
2RH1	1.2	2.0	1.2	_	0.80	0.39
3EML	1.6	2.8	1.6	1.1	_	0.48
1F88	2.4	2.6	2.8	2.1	2.0	_

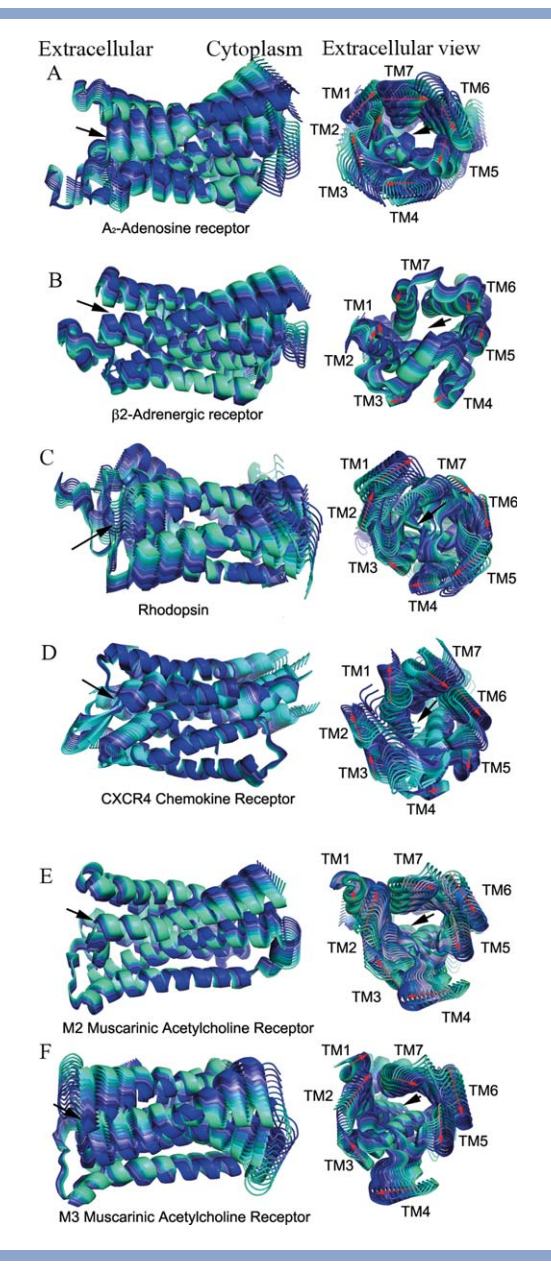


Figure 2

Normal mode dynamics of GPCRs. Shown are the motion exhibited by (A) the A_{2A} -adenosine receptor (PDB ID: 3EML), (B) the β_2 -adrenergic receptor (PDB ID: 2RH1), (C) rhodopsin (PDB ID: 1F88), (D) the CXCR4 chemokine receptor (PDB ID: 3ODU), and (E,F) the M2 and M3 muscarinic acetylcholine receptors, respectively, (PDB ID: 3UON and 4DAJ), associated with the slowest mode calculated using ElNémo. Black arrows indicate the location of the ligand binding site. Red arrows indicate the motion of the numbered TM helices. Distortions along the lowest frequency mode are gradually colored from cyan to blue. Note the contraction of the ligand binding pocket as TM helices come close. The figure was prepared using Pymol.

Å), and TM7 (1 Å) between the active (Gs bound) and inactive (carozolol bound) states of the β_2 adrenergic receptor. 44,45 In addition, our normal mode calculations indicate that contraction of the ligand binding pocket of GPCRs is correlated with expansion of the intracellular

G-protein binding cavity. This is also in agreement with experimental data which shows that constriction of the ligand binding site is correlated with dilation of the Gs binding site in the β₂-adrenergic receptor. ^{44,45} In particular, the intracellular segments of the β₂-adrenergic receptor and especially TM5 (2 Å) and TM6 (14 Å), move apart during receptor activation and thereby expose the Gs binding site on TM3 and TM7 similarly to the motion observed in our normal modes.^{44,45} Normal modes however do not display the extension of TM5 by two helical turns. Thus normal modes may be used as a good indicator of conformational change between active and inactive states. Very often, the slowest normal mode is enough to describe molecular motion in biomole-Here too, the lowest frequency mode describes well the motion of the GPCRs observed experimentally.

Remarkably, the aromatic amino acid cap between the orthosteric site and the ligand binding site is observed to move out of the way so as to allow ligand passage during normal modes. The motion of the aromatic cap sidechain atoms is less than one Angstrom (data not shown), albeit not as large as that measured experimentally. 44,45 The discrepancy in size is due to the fact, that experimental motion of the aromatic cap is localized to the side-chain and less to the backbone, and normal mode motion concentrates on backbone motion.

Cartesian versus polar coordinates

In this study, we calculated normal modes using various techniques to test the robustness of the results. The various techniques yielded similar results, and we did not find any major difference using Cartesian coordinates techniques. The C_α RMSD of the slowest mode calculated using Cartesian coordinate techniques, ElNémo and Nomad-Ref, display a correlation coefficient close to 1. Torsion angle normal modes also yield similar results except their order is switched, and the average correlation coefficient of their C_{α} displacement is 0.77. The major difference between Cartesian and polar coordinates is the relative amplitude of motion along the polypeptide chain. Also, normal modes calculated using polar coordinates do not suffer from the "tip effect" of Cartesian space in which peptide segments sticking out of the protein, such as long surface loops, and long disordered termini display large amplitude motions. More about the differences and similarities of normal modes in Cartesian and torsion angle space has been reviewed by Levitt and coworkers.

Motion of the third intracellular loop

Normal modes were also calculated for GPCR with the third intracellular loop replaced by T4 lysozyme (T4L) as in the original X-ray structures (data not shown). These

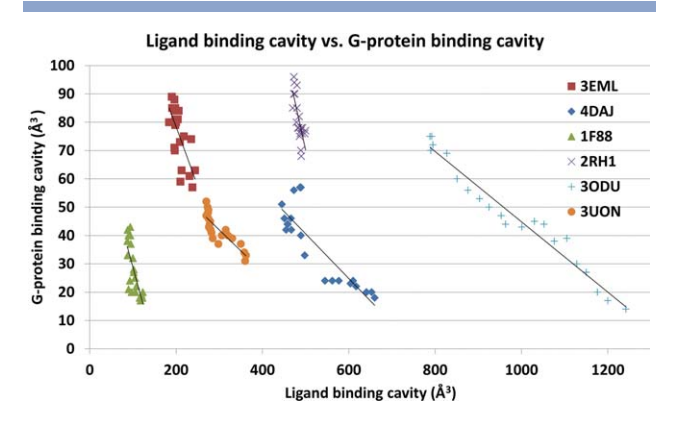


Figure 3

Volume of GPCR ligand binding pocket and G-protein binding pocket. Shown is a plot of the volume of the ligand binding site against the volume of the intracellular G-protein binding cavity of the M2 and M3 muscarinic acetylcholine receptors (PDB ID: 3UON and 4DAJ), the β₂adrenergic receptor (PDB ID: 2RH1), the A2A-adenosine receptor (PDB ID: 3EML), the CXCR4 chemokine receptor (PDB ID: 3ODU), and rhodopsin (PDB ID: 1F88) associated with the slowest mode calculated using ElNémo. Gradual contraction of the ligand binding pocket is correlated with expansion of the G-protein binding pocket.

calculations exhibit a large tilt and roll of the lysozyme domain in relation to the membrane plane. The tilt and roll of T4L is illustrative of the flexibility and conformational agility associated with the third intracellular loop, that upon activation adopts α -helical conformation to elongate TM5 and TM6.44,45 Tilting of the third intracellular loop of the receptor is mechanically associated with ligand binding and induced by vestibule contraction through normal modes. Finally, the tilt and elongation generates a binding cavity for the G-protein.

Ligand binding cavity is inversely correlated with G-protein binding cavity

Figure 3 plots the size of the ligand binding site and passageway against the size of the intracellular G-protein binding cavity as calculated using the slowest mode of ElNémo. The data suggest an inverse correlation between the volumes of the ligand binding site and the G-protein cavity. The inverse correlation holds for all GPCRs tested. The inverse correlation was also found by Bahar and coworkers³⁵ for rhodopsin. The inverse correlation is more pronounced in GPCRs with large initial ligand binding cavity, such as the CXCR4 receptor (PDB ID: 3ODU) which must accommodate a large SDF-1 protein ligand. Contrarily, rhodopsin (PDB ID: 1F88) which accommodates a covalently bound ligand displays a small and little changing binding cavity, as the vestibule is filled with the chromophore lid. In between these extremes, the cavities of the β₂-adrenergic receptor, A_{2A}adenosine receptor, and M2 and M3 muscarinic receptor show a moderate size change of their ligand binding cavities.

Since the real motion is a linear combination of all normal modes, and correlated motion may not be deduced from one mode alone, 48 we tested the positive correlation between contraction of the ligand binding site and dilation of the G-protein binding site in the 25 lowest modes of PDB ID 3UON. Our results indicate that in modes 7-15, 18-20, and 23 the motion is correlated to different degrees. In modes 16-17, 21-22, and 24-25, the motion was not correlated, and in none of the modes was the motion anti-correlated. Since most conformational changes are described by the large amplitude low-frequency modes, 24,49,50 then we may conclude, that contraction of the ligand binding pocket and expansion of the G-protein binding pocket are positively correlated.

Rhodopsin is unsuited to represent the motion of the GPCR family

In a recent study, the principal component analysis (PCA) of 16 X-ray structures of rhodopsin was performed and compared with normal modes using the anisotropic network model.⁴⁷ Interestingly, the PCA modes superbly clustered the inactive rhodopsin structures and the putative activated opsin structures into two separate groups. The normal mode motion displayed by rhodopsin in that study is in agreement with those of rhodopsin calculated herein. However, the slowest modes of rhodopsin are different from those displayed by the other GPCR members (Table I). Shown in Table I, are the correlation coefficients for the C_{α} displacement (RMSD, upper right triangle) of the slowest modes and the C_{α} root mean square deviation (RMSD, lower left triangle) of the various GPCRs, 3UON (M2 muscarinic acetylcholine receptor), 4DAJ (M3 muscarinic acetylcholine receptor), 2RH1 (β₂-adrenergic receptor), 3EML (A_{2A}adenosine receptor), 3ODU (CXCR4 chemokine receptor), and 1F88 (rhodopsin).

It is interesting to note that all GPCRs (but rhodopsin) display an average correlation of ~ 0.8 for their C_{α} displacement value RMSD For rhodopsin however, none of the five lowest frequency normal modes display any correlation of C_{α} displacement RMSD above 0.5. The rhodopsin modes did not appear to be linear combinations of modes of other GPCRs either. This lack of correlation is mainly due to dissimilarities and a low RMSD of the initial X-ray structures (note the large and consistent Co RMSD of rhodopsin with its GPCR neighbors in Table I which are inversely correlated with the RMSD of motion), and in particular the presence of a β-strand lid of the retinal chromophore. This lid seems to lock together adjacent TM helices, and does not allow for the full opening of the ligand binding site. This is particular evident in Figure 1, in which the extracellular ends of the TM1 and TM2 helices display less motion than other GPCRs. Also, TM5 and TM6 motion and in particular

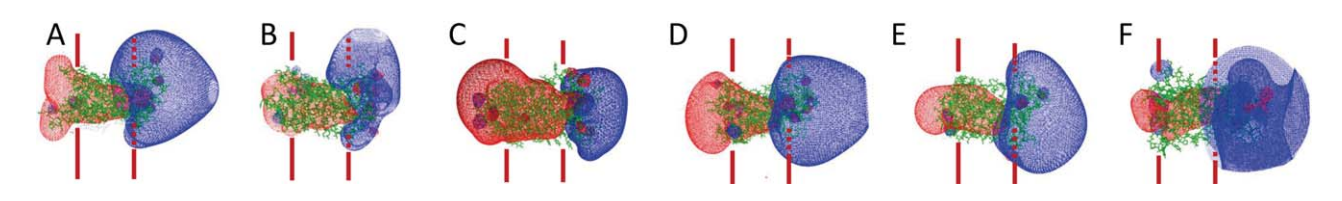


Figure 4

Electrostatic potential of GPCRs. Shown is the Poisson-Boltzmann electrostatic potential of (A) the A_{2A}-adenosine receptor (PDB ID: 3EML), (B) the β₂-adrenergic receptor (PDB ID: 2RH1), (C) rhodopsin (PDB ID: 1F88), (D) the CXCR4 chemokine receptor (PDB ID: 3ODU), and (E,F) the M2 and M3 muscarinic acetylcholine receptors, respectively (PDB ID: 3UON and 4DAJ). Note the negatively charged electrostatic field (in red) protruding from the ligand binding site of the receptor, and the positively charged field (in blue) emanating from the G-protein binding site. The figure was prepared using VMD.⁴²

the third intracellular loop seems to be larger in rhodopsin than in other GPCR. These fluctuations attest to the fact that the rhodopsin structure is unsuited to represent the motion and dynamics of the GPCR family in drug discovery.

Electrostatic potential

The electrostatic potential calculated using Poisson-Boltzmann equations of several GPCRs is shown in Figure 4. Remarkably, the electrostatic potential shows a negatively charged field protruding several nanometers away from the negatively charge membrane phospholipids and into the synaptic cleft. This protruding field is similar to that of other receptor that bind positively charged ligands such as the acetylcholine esterase,⁵¹ the acetylcholine binding protein,⁵² and the nicotinic acetylcholine receptor.⁵³ The negatively charged electrostatic field attracts positively charged neurotransmitters (i.e., acetylcholine) diffusing across the synaptic cleft. In the GPCRs shown in Figure 4, the protruding electrostatic field acts as a concentrated electrostatic siphons on the already negatively charged phospholipid membranes to attract positively charged neurotransmitters, such as muscarine, norepinephrine, and adenosine at physiological conditions (Fig. 5).

Proline hinge of GPCRs

Several studies show the importance of the conserved proline residue that break the TM helices (Ref. 1 and references therein). These prolines act as pivotal hinges inside the GPCRs (Fig. 5), and ensure the efficient propagation of signals from the extracellular to the intracellular domains. This effect was already noted by Bahar and coworkers, 35 and shown to be important for signal propagation in rhodopsin. This effect is reminiscent of that dubbed the "toggle-switch" activation model in which TM6 and TM7 perform "vertical" see-saw movements around the conserved proline bends to explain the opposite directed movements of the TMs at the intraand extracellular ends.⁵⁴ In our study, the "vertical" seesaw movement is not observed, and TM6 and 7 become

exposed as result of a conformational change. Figure 5 emphasizes the importance of the TM proline residues and attest to the strength of normal modes in calculating conformational changes.

DISCUSSION

Normal modes provide a very detailed description of the long term dynamics around a local energy minimum. As such, these data provide a reasonable insight into the activation mechanism of GPCR. In this article, we focus on the motion of the lowest frequency normal mode, as it shows a clear correlation between motion of the binding site and of the cytoplasmic domain. This however does not mean that higher frequency normal modes are not representative of the motion of GPCR. High frequency normal modes show bending and local motion in either the binding site or the cytoplasmic domain, but do not necessarily correlate between the vestibule contraction and the cavity expansion or tilting of the cytoplasmic T4L. Furthermore, bending motion is strongly

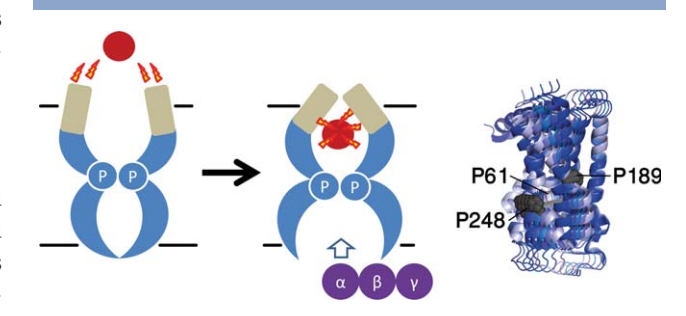


Figure 5

Schematic illustration of GPCR activation mechanism. Extracellular ligand binding (in red) is engendered through electrostatic attraction. Ligand binding leads to contraction of the ligand binding pocket, and expansion of the intracellular G-protein (in purple) binding cavity. Note that the balls noted "P" represent the conserved proline residues of GPCRs, which correspond to P61, P189, and P249 of the A2A-adenosine receptor (PDB ID: 3EML) shown on the right. These proline residues, located on the TM helices serve as hinges to propagate the motion from the extracellular to the intracellular domains. This mechanism of activation is proposed through normal modes analysis.

hindered by the presence of surrounding lipid molecules as noted by Bahar and coworkers.³⁵ On the basis of these results, we concluded that this is the most robust mechanism of motion, and we reported the results based on this mode.

Caveats

For simplicity, the molecular activation mechanism of GPCRs is discussed as if there was only one active conformation, which is most probably not the case (for review, see Ref. 1). Any GPCR may even be found in the same membrane in different active conformation states and activating different G-proteins. However, in the context of this study, it is expected that such different active conformations constitute minor variations of the main activation mechanism proposed herein.

Oligomerization state of GPCRs

Several GPCRs have been reported to form homo- and heterooligomers. For instance, CXCR4 has a propensity to form hetero- and homooligomers, 55 and such oligomerization could play a role in the allosteric regulation of GPCR signaling.⁵⁶ The oligomerization state however, does not preclude the activation mechanisms proposed herein. In fact, normal mode analysis of dimers of the CXCR4 (data not shown) displays the correlated contraction of the extracellular domain, and dilation of the G-protein binding cavity.

Mechanism of action

The lowest frequency mode is often sufficient to explain the conformational changes and mechanical motion in proteins thus attesting to the robustness of elastic network normal modes.^{29,30} Also here, the lowest frequency normal mode exposes the conformational change induced by ligand binding as described earlier.

The normal mode induced conformational changes of the β₂-AR are very similar to those observed between the inactive and active state of the X-ray structure. 44 In the normal G-protein cycle, extracellular agonist binding to the receptor leads to conformational rearrangements of the cytoplasmic ends of transmembrane segments that enable the G-protein heterotrimer $(\alpha, \beta, \text{ and } \gamma)$ to bind the receptor. GDP is released from the α subunit upon formation of G-protein receptor complex. The GTP binds to the nucleotide-free α subunit resulting in dissociation of the α and $\beta \gamma$ subunits from the receptor. The subunits regulate their respective effector proteins adenylyl cyclase (AC) and Ca²⁺ channels. In the end, the G-protein heterotrimer reassembles from α and $\beta\gamma$ subunits following hydrolysis of GTP to GDP in the α subunit.

From the X-ray structures, it is clear that opening of the helical bundle is a critical event for binding and activation of G-protein, transducin, by generating a cavity that provides sufficient volume for interaction and exposing resi-

dues involved in binding. In addition, helical elongation of TM5 and TM6 is also a critical event for G-protein binding. Both of these observed events, are found through elastic network normal mode in this study. This study suggests that beyond these two events, the overall torsional motion of the TM domains, that simultaneously induces the dilation of the extracellular binding site and the constriction of the intracellular G-protein binding cavity, underlies the conformational transitions.

ACKNOWLEDGEMENTS

The authors thank Prof. Michael Levitt for careful reading of the manuscript.

REFERENCES

- 1. Schwartz TW, Frimurer TM, Holst B, Rosenkilde MM, Elling CE. Molecular mechanism of 7TM receptor activation—a global toggle switch model. Annu Rev Pharmacol Toxicol 2006;46:481-519.
- 2. Gether U. Uncovering molecular mechanisms involved in activation of G protein-coupled receptors. Endocr Rev 2000;21:90-113.
- 3. Haga K, Kruse AC, Asada H, Yurugi-Kobayashi T, Shiroishi M, Zhang C, Weis WI, Okada T, Kobilka BK, Haga T, Kobayashi T. Structure of the human M2 muscarinic acetylcholine receptor bound to an antagonist. Nature 2012;482:547-551.
- 4. Kruse AC, Hu J, Pan AC, Arlow DH, Rosenbaum DM, Rosemond E, Green HF, Liu T, Chae PS, Dror RO, Shaw DE, Weis WI, Wess J, Kobilka BK. Structure and dynamics of the M3 muscarinic acetylcholine receptor. Nature 2012;482:552-556.
- 5. Wu B, Chien EY, Mol CD, Fenalti G, Liu W, Katritch V, Abagyan R, Brooun A, Wells P, Bi FC, Hamel DJ, Kuhn P, Handel TM, Cherezov V, Stevens RC. Structures of the CXCR4 chemokine GPCR with small-molecule and cyclic peptide antagonists. Science 2010:330:1066-1071.
- 6. Jaakola VP, Griffith MT, Hanson MA, Cherezov V, Chien EY, Lane JR, Ijzerman AP, Stevens RC. The 2.6 angstrom crystal structure of a human A2A adenosine receptor bound to an antagonist. Science 2008:322:1211-1217.
- 7. Cherezov V, Rosenbaum DM, Hanson MA, Rasmussen SG, Thian FS, Kobilka TS, Choi HJ, Kuhn P, Weis WI, Kobilka BK, Stevens RC. High-resolution crystal structure of an engineered human beta2-adrenergic G protein-coupled receptor. Science 2007;318:
- 8. Hulme EC, Birdsall NJ, Buckley NJ. Muscarinic receptor subtypes. Annu Rev Pharmacol Toxicol 1990;30:633-673.
- 9. Moser B, Wolf M, Walz A, Loetscher P. Chemokines: multiple levels of leukocyte migration control. Trends Immunol 2004;25:75-84.
- 10. Fulton AM. The chemokine receptors CXCR4 and CXCR3 in cancer. Curr Oncol Rep 2009;11:125-131.
- 11. Feng Y, Broder CC, Kennedy PE, Berger EA. HIV-1 entry cofactor: functional cDNA cloning of a seven-transmembrane, G proteincoupled receptor. Science 1996;272:872-877.
- 12. Taylor MR. Pharmacogenetics of the human beta-adrenergic receptors. Pharmacogen J 2007;7:29-37.
- 13. Dunwiddie TV, Masino SA. The role and regulation of adenosine in the central nervous system. Annu Rev Neurosci 2001;24:31-55.
- 14. Palczewski K, Kumasaka T, Hori T, Behnke CA, Motoshima H, Fox BA, Le Trong I, Teller DC, Okada T, Stenkamp RE, Yamamoto M, Miyano M. Crystal structure of rhodopsin: a G protein-coupled receptor. Science 2000;289:739-745.
- 15. Palczewski K. G protein-coupled receptor rhodopsin. Annu Rev Biochem 2006;75:743-767.

- 16. Brooks B, Karplus M. Harmonic dynamics of proteins: normal modes and fluctuations in bovine pancreatic trypsin inhibitor. Proc Natl Acad Sci USA 1983;80:6571-6575.
- 17. Levitt M, Sander C, Stern PS. Protein normal-mode dynamics: trypsin inhibitor, crambin, ribonuclease and lysozyme. J Mol Biol 1985; 181:423-447.
- 18. Go N, Noguti T, Nishikawa T. Dynamics of a small globular protein in terms of low-frequency vibrational modes. Proc Natl Acad Sci USA 1983;80:3696-3700.
- 19. Tirion MM. Large amplitude elastic motions in proteins from a single-parameter, atomic analysis. Phys Rev Lett 1996;77:1905-1908.
- 20. Delarue M, Sanejouand YH. Simplified normal mode analysis of conformational transitions in DNA-dependent polymerases: the elastic network model. J Mol Biol 2002;320:1011-1024.
- 21. Hinsen K. Analysis of domain motions by approximate normal mode calculations. Proteins 1998;33:417-429.
- 22. Doruker P, Atilgan AR, Bahar I. Dynamics of proteins predicted by molecular dynamics simulations and analytical approaches: application to alpha-amylase inhibitor. Proteins 2000;40:512-524.
- 23. Atilgan AR, Durell SR, Jernigan RL, Demirel MC, Keskin O, Bahar I. Anisotropy of fluctuation dynamics of proteins with an elastic network model. Biophys J 2001;80:505-515.
- 24. Tama F, Sanejouand YH. Conformational change of proteins arising from normal mode calculations. Protein Eng 2001;14:1-6.
- 25. Eyal E, Yang LW, Bahar I. Anisotropic network model: systematic evaluation and a new web interface. Bioinformatics 2006;22:2619-
- 26. Suhre K, Sanejouand YH. ElNemo: a normal mode web server for protein movement analysis and the generation of templates for molecular replacement. Nucleic Acids Res 2004;32:W610-W614.
- 27. van der Spoel D, Lindahl E, Hess B, Groenhof G, Mark AE, Berendsen HJ. GROMACS: fast, flexible, and free. J Comput Chem 2005;26:1701-1718.
- 28. Lindahl E, Azuara C, Koehl P, Delarue M. NOMAD-Ref: visualization, deformation and refinement of macromolecular structures based on all-atom normal mode analysis. Nucleic Acids Res 2006; 34:W52-W56.
- 29. Samson AO, Levitt M. Normal modes of prion proteins: from native to infectious particle. Biochemistry 2011;50:2243-2248.
- 30. Samson AO, Levitt M. Inhibition mechanism of the acetylcholine receptor by alpha-neurotoxins as revealed by normal-mode dynamics. Biochemistry 2008;47:4065-4070.
- 31. Taly A, Corringer PJ, Grutter T, Prado de Carvalho L, Karplus M, Changeux JP. Implications of the quaternary twist allosteric model for the physiology and pathology of nicotinic acetylcholine receptors. Proc Natl Acad Sci USA 2006;103:16965-16970.
- 32. Bahar I, Lezon TR, Yang LW, Eyal E. Global dynamics of proteins: bridging between structure and function. Annu Rev Biophys 2010; 39:23-42.
- 33. Niv MY, Skrabanek L, Filizola M, Weinstein H. Modeling activated states of GPCRs: the rhodopsin template, J Comput Aided Mol Des 2006;20:437-448.
- 34. Kim JE, Tauber MJ, Mathies RA. Analysis of the mode-specific excited-state energy distribution and wavelength-dependent photoreaction quantum yield in rhodopsin. Biophys J 2003;84:2492-2501.
- 35. Isin B, Rader AJ, Dhiman HK, Klein-Seetharaman J, Bahar I. Predisposition of the dark state of rhodopsin to functional changes in structure. Proteins 2006;65:970-983.
- 36. Isin B, Schulten K, Tajkhorshid E, Bahar I. Mechanism of signal propagation upon retinal isomerization: insights from molecular dynamics simulations of rhodopsin restrained by normal modes. Biophys J 2008;95:789-803.
- 37. Niv MY, Filizola M. Influence of oligomerization on the dynamics of G-protein coupled receptors as assessed by normal mode analysis. Proteins 2008;71:575-586.

- 38. Bahar I, Lezon TR, Bakan A, Shrivastava IH. Normal mode analysis of biomolecular structures: functional mechanisms of membrane proteins. Chem Rev 2010;110:1463-1497.
- 39. Thompson JD, Higgins DG, Gibson TJ. CLUSTAL W: improving the sensitivity of progressive multiple sequence alignment through sequence weighting, positions-specific gap penalties and weight matrix choice. Nucl Acids Res 1994;22:4673-4680.
- 40. Huang B, Schroeder M. LIGSITEcsc: predicting ligand binding sites using the Connolly surface and degree of conservation. BMC Struct Biol 2006;6:19.
- 41. Konecny R, Baker NA, McCammon JA. iAPBS: a programming interface to Adaptive Poisson-Boltzmann Solver (APBS). Comput Sci Discov 2012;5(1).
- 42. Humphrey W, Dalke A, Schulten K. VMD: visual molecular dynamics, J Mol Graph 1996;14:27-38.
- 43. Bray JK, Weiss DR, Levitt M. Optimized torsion-angle normal modes reproduce conformational changes more accurately than cartesian modes. Biophys J 2011;101:2966-2969.
- 44. Rasmussen SG, DeVree BT, Zou Y, Kruse AC, Chung KY, Kobilka TS, Thian FS, Chae PS, Pardon E, Calinski D, Mathiesen JM, Shah ST, Lyons JA, Caffrey M, Gellman SH, Steyaert J, Skiniotis G, Weis WI, Sunahara RK, Kobilka BK. Crystal structure of the beta2 adrenergic receptor-Gs protein complex. Nature 2011;477:549-555.
- 45. Chung KY, Rasmussen SG, Liu T, Li S, DeVree BT, Chae PS, Calinski D, Kobilka BK, Woods VL, Jr, Sunahara RK. Conformational changes in the G protein Gs induced by the beta2 adrenergic receptor. Nature 2011;477:611-615.
- 46. Krebs WG, Alexandrov V, Wilson CA, Echols N, Yu H, Gerstein M. Normal mode analysis of macromolecular motions in a database framework: developing mode concentration as a useful classifying statistic. Proteins 2002;48:682-695.
- 47. Bahar I. On the functional significance of soft modes predicted by coarse-grained models for membrane proteins. J Gen Physiol 2010; 135:563-573.
- 48. Van Wynsberghe AW, Cui Q. Interpreting correlated motions using normal mode analysis. Structure 2006;14:1647-1653.
- 49. Cui Q, Li G, Ma J, Karplus M. A normal mode analysis of structural plasticity in the biomolecular motor F(1)-ATPase. J Mol Biol 2004; 340:345-372.
- 50. Petrone P, Pande VS. Can conformational change be described by only a few normal modes? Biophys J 2006;90:1583-1593.
- 51. Harel M, Schalk I, Ehret-Sabatier L, Bouet F, Goeldner M, Hirth C, Axelsen PH, Silman I, Sussman JL. Quaternary ligand binding to aromatic residues in the active-site gorge of acetylcholinesterase. Proc Natl Acad Sci USA 1993;90:9031-9035.
- 52. Brejc K, van Dijk WJ, Klaassen RV, Schuurmans M, van Der Oost J, Smit AB, Sixma TK. Crystal structure of an ACh-binding protein reveals the ligand-binding domain of nicotinic receptors. Nature 2001;411:269-276.
- 53. Samson A, Scherf T, Eisenstein M, Chill J, Anglister J. The mechanism for acetylcholine receptor inhibition by alpha-neurotoxins and species-specific resistance to a-bungarotoxin revealed by NMR. Neuron 2002;35:319-332.
- 54. Elling CE, Frimurer TM, Gerlach LO, Jorgensen R, Holst B, Schwartz TW. Metal ion site engineering indicates a global toggle switch model for seven-transmembrane receptor activation. J Biol Chem 2006;281:17337-17346.
- 55. Babcock GJ, Farzan M, Sodroski J. Ligand-independent dimerization of CXCR4, a principal HIV-1 coreceptor. J Biol Chem 2003;278: 3378-3385.
- 56. Wang J, Norcross M. Dimerization of chemokine receptors in living cells: key to receptor function and novel targets for therapy. Drug Discov Today 2008;13:625-632.